GEOLOGICA CARPATHICA, APRIL 2014, 65, 2, 147–161 doi: 10.2478/geoca-2014-0010

The recent fault kinematics in the westernmost part of the Getic nappe system (Eastern Serbia): Evidence from fault slip and focal mechanism data

ANA MLADENOVIĆ[1], BRANISLAV TRIVIĆ[1], MILORAD ANTIĆ[2], VLADICA CVETKOVIĆ[1], RADMILA PAVLOVIĆ[1], SLAVICA RADOVANOVIĆ[3] and BERNHARD FÜGENSCHUH[4]

[1]University of Belgrade, Faculty of Mining and Geology, Đušina 7, 11000 Belgrade, Serbia; ana.mladenovic@rgf.bg.ac.rs
[2]Geologisch-Paläontologisches Institut, Universität Basel, Bernoullistrasse 32, 4056 Basel, Switzerland; m.antic@unibas.ch
[3]Seismological Survey of Serbia, Tašmajdanski park bb, Poštanski fah 16, 11120 Belgrade, Serbia; slavica.radovanovic@seismo.gov.rs
[4]Geology and Paleontology, Innsbruck University, Innrain 52f, A-6020 Innsbruck, Austria; bernhard.fuegenschuh@uibk.ac.at

(Manuscript received October 22, 2013; accepted in revised form March 11, 2014)

Abstract: In this study we performed a calculation of the tectonic stress tensor based on fault slip data and all available focal mechanisms in order to determine the principal stress axes and the recent tectonic regime of the westernmost unit of the Getic nappe system (Gornjak-Ravanica Zone, Eastern Serbia). The study is based on a combined dataset involving paleostress analyses, the inversion of focal mechanisms and remote sensing. The results show dominant strike-slip kinematics with the maximal compression axis oriented NNE–SSW. This is compatible with a combined northward motion and counterclockwise rotation of the Adria plate as the controlling factor. However, the local stress field is also shown to be of great importance and is superimposed on the far-field stress. We managed to distinguish three areas with distinct seismic activity. The northern part of the research area is characterized by transtensional tectonics, possibly under the influence of the extension in the areas situated more to the northeast. The central and seismically most active part is dominated by strike-slip tectonics whereas the southern area is slightly transpressional, possibly under the influence of the rigid Moesian Platform situated to the east of the research area. The dominant active fault systems are oriented N–S (to NE–SW) and NW–SE and they occur as structures of either regional or local significance. Regional structures are active in the northern and central part of the study area, while the active fault systems in the southern part are marked as locally important. This study suggests that seismicity of this area is controlled by the release of accumulated stress at local accommodation zones which are favourably oriented in respect to the active regional stress field.

Key words: Fault-plane solutions, paleostress, recent stress field, Getic nappe, East Serbia.

Introduction

The East Serbian part of the Carpatho-Balkanides comprises a geodynamically complex zone which present-day structural pattern is a result of Late Cretaceous subduction of the Vardar zone below the 'European' units, followed by Cenozoic post-collisional and neotectonic phases, namely extension and younger transpression (e.g. Cvetković et al. 2004; Karamata 2006; Bada et al. 2007; Schmid et al. 2008) (Fig. 1). Since the Late Miocene, the most important factor controlling regional tectonic processes in this area has been the counterclockwise rotation and northward motion of the Adriatic microplate in respect to the Dinaric orogen (e.g. Ustaszewski et al. 2008). In the Carpatho-Balkanides this motion is generally manifested through moderate to weak but constant seismicity with stronger earthquakes recorded mostly along well-known fault systems that were active in the neotectonic period (since the Late Miocene) (Marović et al. 2002b; Bada et al. 2007).

Recent fault kinematics in this part of the Carpatho-Balkan orogenic system are poorly documented. Several regional studies, mostly including the Pannonian Basin or the northern junction between the Getic and Danubian units (easternmost part of Dacia) in Romania (see Schmid et al. 2008 and references therein), were predominantly focused on determining the general geodynamic evolution of the Carpatho-Balkan-Pannonian region. The main conclusions considering the Late Cretaceous-Cenozoic geodynamic evolution of the Getic-Supragetic nappe system, as a major part of the Carpatho-Balkanides in East Serbia, can be summarized by three deformation phases (Matenco & Schmid 1999): (1) the Late Cretaceous NNW-SSE contraction, (2) the Paleogene to Early Miocene SSE-NNW extension, and (3) the Late Miocene tectonics related predominantly to strike slip movements.

The youngest deformation phase occurred in Late Miocene-Pliocene times and it is also related to the present day stress field (Horvath & Cloetingh 1996; Marović et al. 2002b; Bada et al. 2007). It is characterized by strike-slip tectonics mainly caused by SW compression (Horvath & Cloetingh 1996; Marović et al. 2002b; Bada et al. 2007). This state of the stress field is evident through a regional phase of inversion of the Pannonian Basin (e.g. Bada et al. 2007). The major tectonic forces responsible for this stress field are related to the counterclockwise rotation and northward motion of the Adriatic microplate ('Adria push'), and this is also evident from earlier studies in the Pannonian Basin and its immediate surroundings (Gerner et al. 1999; Marović

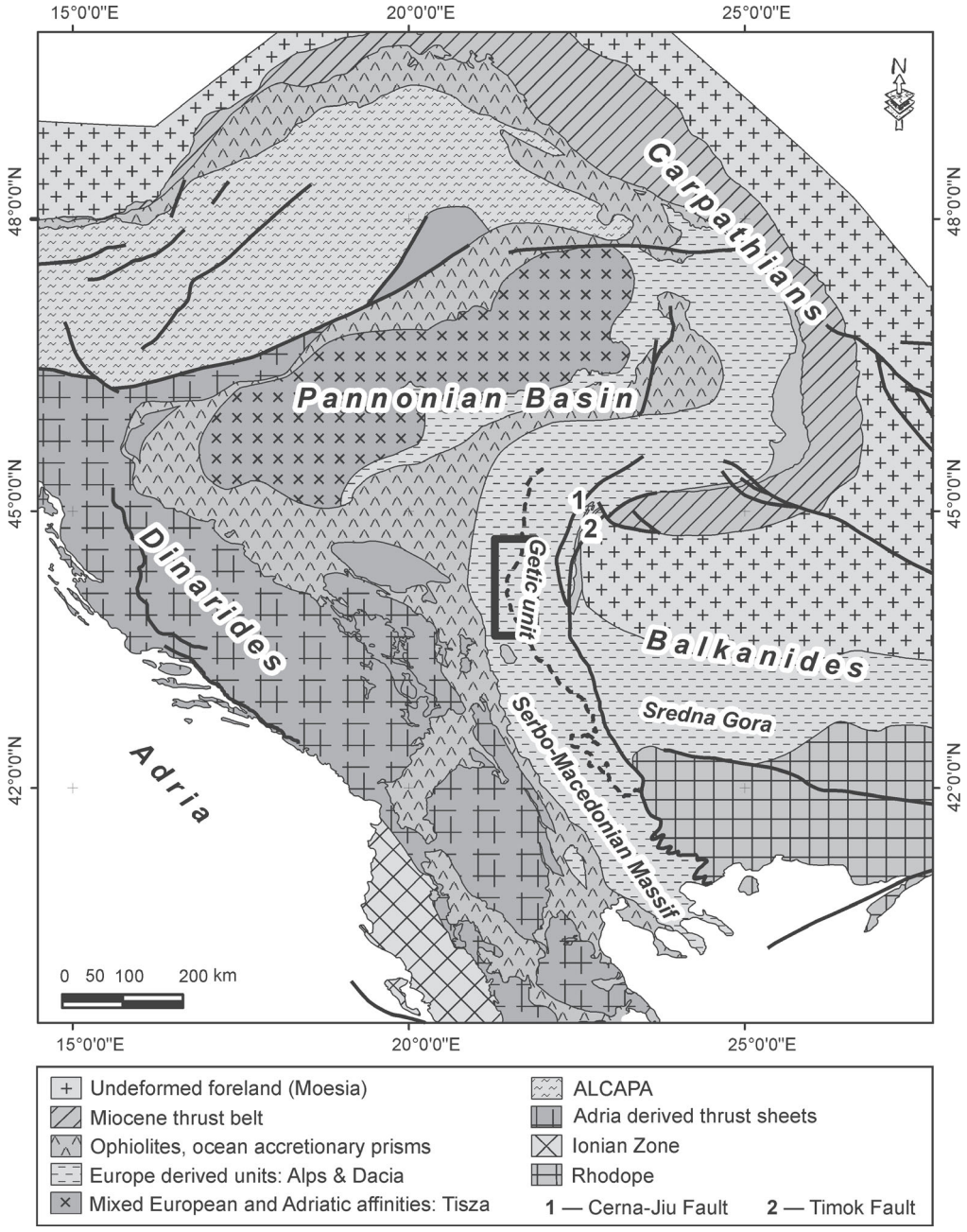

Fig. 1. Schematic geotectonic position of the research area (after Schmid et al. 2008). The dashed line represents the boundary between the Serbo-Macedonian Massif and the Getic unit in the territory of southwesternmost Romania, eastern and southeastern Serbia and western Bulgaria.

et al. 2002b; Grenerczy & Bada 2005; Bada et al. 2007). The contact between the Serbo-Macedonian Massif and Carpatho-Balkanides was either omitted or only partly included in these regional studies, therefore, detailed information about Miocene to recent tectonics of this tectonic zone is missing. Although some studies do exist (Radovanović & Pavlović 1992; Radovanović & Pavlović 1994; Marović et al. 2002b), they focus on small areas and are not integrated into the existing regional models (e.g. Horvath & Cloetingh 1996; Bada et al. 2007).

The main aim of this research is to better constrain the late Miocene to recent stress field of the western part of the East Serbian Carpatho-Balkanides by combining fault slip data and focal mechanisms. The paleostress analysis of fault-slip data (PSA) was performed on a number of fault planes with different slip sense and containing multiple slip indicators (e.g. striations). In this study only the youngest fault planes were used, whereas the whole paleostress analysis, covering brittle tectonic events from the Upper Cretaceous till recent times, will be published in a separate paper. The fault-slip data are integrated with the results of a focal mechanism analysis (FMA) which included a systematic study of all available earthquakes that happened in this part of the Carpatho-Balkanides since 1983. Our study suggests that there is a strong

correlation between paleostress fault-slip data and data obtained by inversion of focal mechanisms and that this correlation can be generally used in elucidating the link between the last tectonic phases and recent stress-field conditions.

Geotectonic setting

The research area is located within the westernmost part of the Getic nappe system along its contact with the Supragetic and the Serbo-Macedonian units (Fig. 2). Generally, these geotectonic entities are derived from the Dacia Mega unit (Schmid et al. 2008) or Bucovinian-Getic microplate (Kräutner & Krstić 2003). Here, the boundary between these units is overlain by a very thick (up to 4 km) Cenozoic sedimentary cover (Marinković et al. 1978).

The Serbo-Macedonian Massif is composed of Upper Proterozoic to Lower Paleozoic volcano-sedimentary rocks metamorphosed under amphibolite facies conditions, and locally cut by granitoid intrusions (Dimitrijević 1963, 1967, 1995). The Supragetic unit belongs to the east-vergent Getic-Supragetic nappe system (Marović 2001; Schmid et al. 2008). It consists of medium to low grade metamorphic rocks intruded by early Paleozoic granitoids (Veselinović et al. 1970; Kalenić et al. 1980). The Supragetic unit was thrust eastward (in present-day geographical coordinates) over the Getic nappe system during the late early Cretaceous (Dimitrov 1931; Bonchev 1936; Zagorchev & Ruseva 1982; Kounov et al. 2010). This contact can be observed on several localities near Despotovac (Fig. 2, 2 — Morava roof thrust of the Getic unit). The entire Getic-Supragetic nappe system is interpreted as having been formed in mid-Cretaceous times ('Austrian phase') (Matenco & Schmid 1999; Schmid et al. 2008). During the Late Cretaceous 'Laramian' episode this nappe stack has been thrust onto the Danubian units after the closure of the Ceahlau-Severin Ocean (Matenco & Schmid 1999).

The immediate research area is situated within the Getic unit which represents a single tectonic entity since the Paleogene. Here, the Getic unit is composed of several zones representing diverse pre-Cenozoic paleogeographic domains: Proterozoic-Paleozoic basement, Jurassic-Cretaceous sedimentary cover, Senonian tectonic trough and Gornjak-Ravanica Zone (Dimitrijević 1995).

The basement consists of Proterozoic migmatites, gneisses, and micaschists metamorphosed under amphibolite facies conditions as well as of Paleozoic low grade to non-metamorphosed rocks. The whole sequence is intruded by Hercynian I-type granitoids (Gornjane, Brnjica, Neresnica, Kräutner & Krstić 2002). The Jurassic–Cretaceous sedimentary cover transgressively overlies the basement rocks and is in tectonic contact with the Gornjak-Ravanica Zone which is made up of Permian to Jurassic strata. The Senonian trough sediments were deposited within a post-tectonic continental basin postdating the Lower to Mid-Cretaceous main deformation phase of the Getic-Supragetic nappe system (Kräutner & Krstić 2002, 2003; Schmid et al. 2008). The basin is spatially and temporally associated with Turonian–Campanian (92–78 Ma) magmatic activity ("banatites") that resulted from the N-NE-dipping subduction of the Neotethys Ocean further to the south and south-east (Drew 2005; Karamata 2006; Schmid et al. 2008).

The Gornjak-Ravanica Zone (GRZ) (Dimitrijević, 1995) represents the Serbian equivalent of the widespread Saska-Gornjak and Resita units which can be followed from Romania in the north through Serbia up to western Bulgaria in the southeast (Kräutner & Krstić 2003). The GRZ is composed of a thick sequence of red Permian sandstones covered by Triassic and Jurassic limestones. The Mesozoic sediments are intruded by banatites, genetically associated with the Ridanj-Krepoljin fault (Fig. 2, 1 — Ridanj-Krepoljin dislocation). The central part of the Gornjak-Ravanica Zone is affected by the complex Ridanj-Krepoljin dislocation, which also marks the westernmost margin of the Apuseni–Banat–Timok–Srednegorie Magmatic and Metallogenetic Belt in Serbia (e.g. Mitchell 1996; Karamata et al. 1997).

The major present day fault pattern along the East Serbian Carpatho-Balkanides, as shown by Marović et al. (2002a,b), was formed in the Early Miocene and is characterized by NNW–SSE to N–S (NNE–SSW) striking longitudinal faults. The other two fault systems with regional importance have a transversal and diagonal character with respect to the general strike of the tectonic units. Regional importance is attributed to fault systems with significant quantifiable slip at the given scale. Thus, local faults are systems representing secondary structures that accommodate slip exerted on the systems with regional importance.

Methods

This work combines methodologically independent procedures of stress inversion of fault slip data (paleostress analysis) and focal mechanism stress inversion. These procedures are aimed at obtaining the active fault pattern and establishing stress tensors acting in the studied area from the late Miocene (using paleostress analysis) to recent times (by inversion of focal mechanisms). In order to achieve the connection between fault slip data observed in the field on the mesoscale and data on focal mechanisms, which treat regional faults and fault systems on the macro observation scale, a detailed lineament trend analysis was also performed. The lineaments confirmed by field observations and documented on the 1 : 100,000 Geological Map (sheets: Požarevac, Lapovo, Paraćin, Kučevo, Žagubica, Boljevac) are treated as regional faults or fault zones.

Remote Sensing — Lineament trend analyses

The lineament trend analysis was done on satellite images acquired by Landsat 7 ETM+ sensor. Standard procedures for image preprocessing and processing were performed, including spectral image enhancement (brightness and contrast enhancement, normalization of digital number values) and spatial image enhancement (spatial filtering, morphological filtering, and resolution enhancement). Final analysis and interpretation were done on a mosaic of processed satellite images with combined digital elevation model (with 10 m

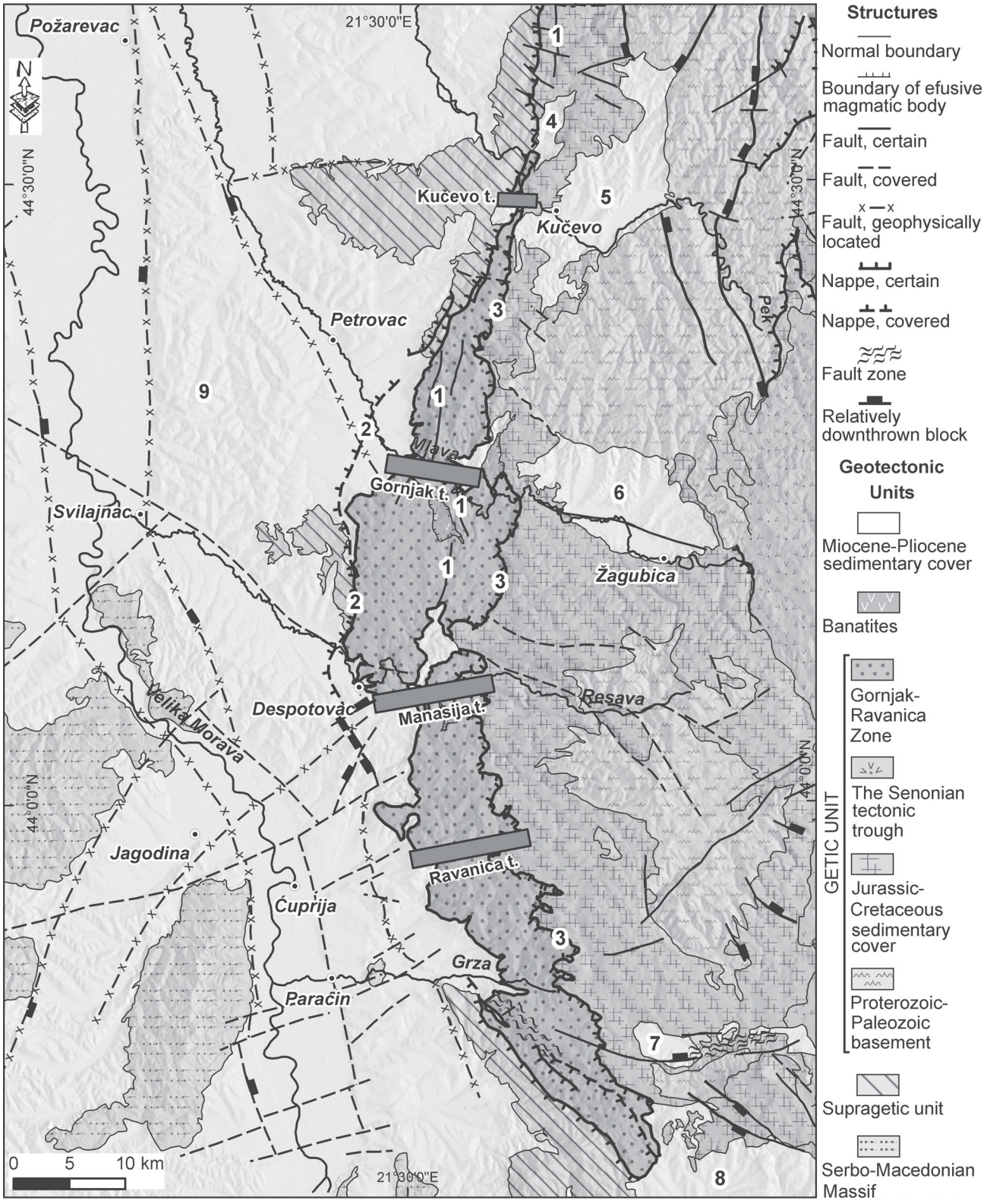

Fig. 2. Simplified tectonic map of the research area, adapted from Basic Geological Map of SFRY 1:100,000, sheets: Požarevac (L34-127), Lapovo (L34-139), Paraćin (K34-007), Kučevo (L34-128), Žagubica (L34-140), Boljevac (K34-008). **1** — Ridanj-Krepoljin dislocation; **2** — Morava roof thrust of SGU. East vergent regional structure, generally oriented from N to S, which represents the tectonic boundary between the SGU and Getic unit; **3** — Red Permian sandstone floor thrust. A major thrust representing the tectonic boundary within two subunits of the Getic Unit; **4** — Rakova Bara Basin; **5** — Kučevo Basin; **6** — Žagubica Basin; **7** — Krivi Vir Basin; **8** — Sokobanja Basin; **9** — Morava Basin.

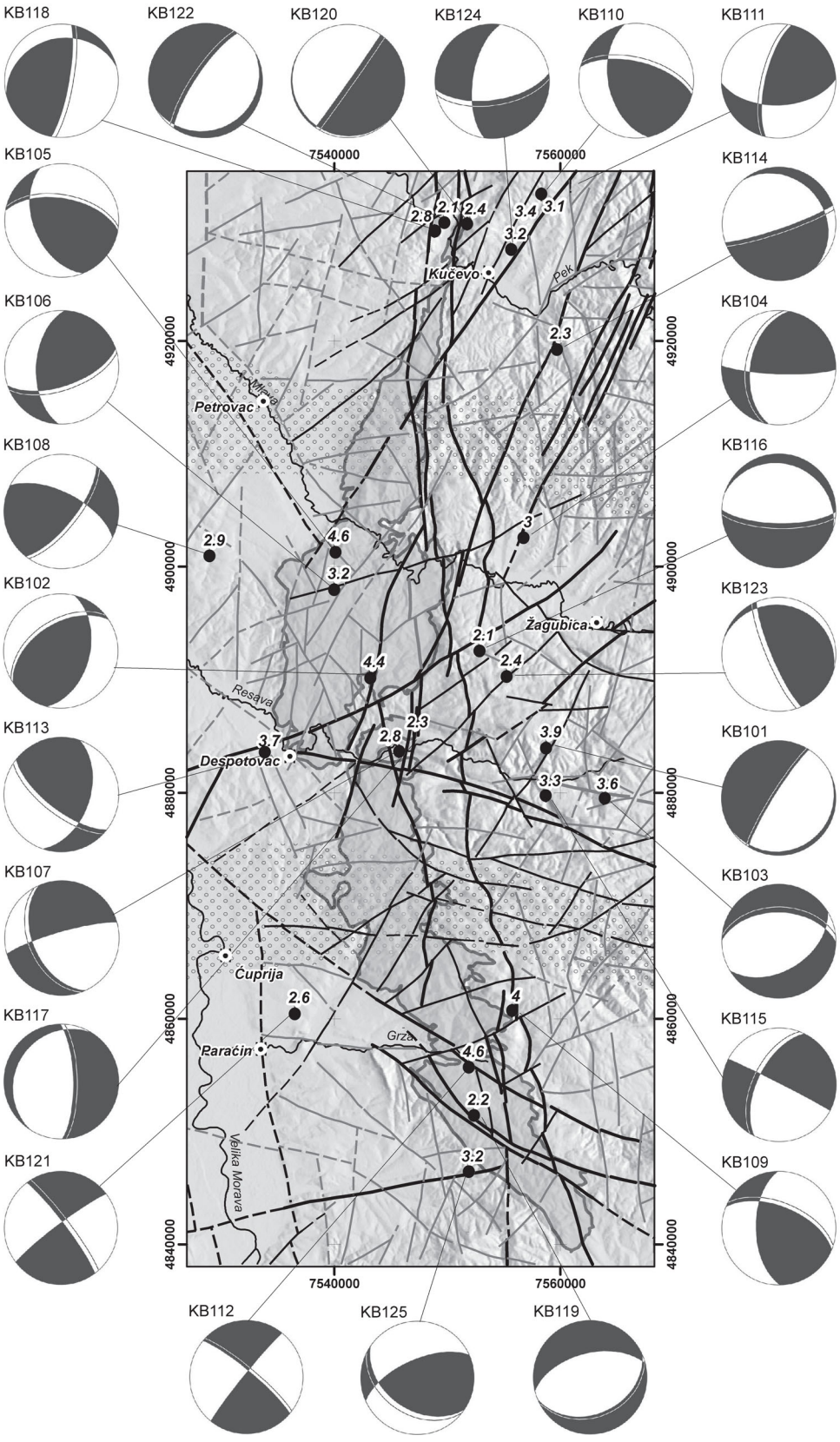

Fig. 3. Map of epicenters and related focal mechanisms (double-line nodal planes on focal plane solutions are regarded as fault planes), and results of the remote sensing lineament trend analysis. Dotted polygons represent areas with low seismic activity. Black lines on remote sensing analysis represent confirmed neotectonic active faults, while grey lines were confirmed only in the field and on geological maps and are not regarded as neotectonically active.

resolution), acquired and processed through ASTER GDEM Project (ASTER GDEM ver. 2).

Standard criteria for determining the position of tectonic lineaments on satellite images were used. Lineament trends were initially proposed on the basis of morphological indicators in the relief. Long and linear river streams, short streams that retain the same direction over watersheds and belong to different drainage systems, sharp changes of direction of streams with the angle of 90 degrees, and abrupt linear and distinct changes in the terrain slope are morphological forms that were used to distinguish possible fault structure from lineaments resulting from lithological differences. Analysis of fault data observed on the field was done regarding their location and orientation of the dominant fault system. Only those tectonic lineaments which correspond to field observed data considering spatial and strike matching are taken into account. The final interpretation was done by incorporating data from the available geological maps (1 : 100,000 Geological Map, sheets: Požarevac, Lapovo, Paraćin, Kučevo, Žagubica, Boljevac).

Analysis of satellite images, by its definition, cannot give information about fault kinematics. However, it was, at least to a certain extent, possible to clarify the neotectonic activity of determined faults. Their clear morphological outline in Pliocene and Quaternary sediments, their continuous orientation along geological units of different age, are certain indicators that these faults were neotectonically active. Taking all these criteria into account, together with literature data (aforementioned geological maps and neotectonic map of Marović et al. 2002a), we produced a map of remote sensing lineament trend analysis (Fig. 3). The faults were classified as regional or local, according to their relative importance in the research area. Lineaments that are featured as regional faults are followed by strike on satellite images. They are clearly visible on a kilometric scale, well documented by field observation and literature data, and they were significant for the brittle tectonic evolution of the research area. The expression in relief of the faults was the criteria for their classification as certain or uncertain (covered).

Paleostress analysis — fault slip stress inversion

Fault-slip data were collected during several field campaigns in 2009 and 2010. The campaigns were carried out along four traverses (from north to south): Kučevo, Gornjak, Manasija and Ravanica (Fig. 2). The majority of faults and fault-slip data were observed in Tithonian reef carbonates (Ravanica Limestone; Dimitrijević 1995). In order to determine the sense of slip on striated fault planes a variety of slip criteria marked as Young Geological Data in the World Stress Map project (Reinecker et al. 2005) were used. The most common linear indicators observed on outcrops were calcite fibers, cataclastic lineation (slickenlines), gouging-grain grooves and "carrot-shaped" markings (Fig. 4). Additionally, slip was determined by observing asymmetric grains, spall marks with congruent steps, lunate fractures, knobby elevations and plucking markings (e.g. Petit 1987; Doblas et al. 1997; Doblas 1998). Only those fault slip measurements with a higher level of quality related to the type of slip indicator were included in the calculations. This is documented in Table 1. Polyphase fault reactivations, which were reflected by superimposed sets of slickensides, are observed at all outcrops. The relative chronology of brittle structures was established solely by the cross-cutting relationships of faults and/or slip indicators. In addition, stress inversion based on focal mechanisms served as a reference frame for the youngest tectonic phase. Therefore, from the collection of paleostress solutions integrated in a succession of tectonic events with established relative age hierarchy, only those defining the youngest stress field are treated in this paper.

Initial separation of data was based on the outcrop location. Subsequent separation was indeed based on slip observed on the given fault and its orientation. Paleostress calculations of data-sets were done using the TectonicsFP software (Ortner et al. 2002), with two approaches: direct inversion method — INV (Angelier 1979) and Numerical Dynamic Analysis — NDA (Spang 1972; Sperner & Ratschbacher 1994) (see Table 1). Direct inversion method was applied to fault data sets with confirmed reactivated slip along the pre-existing faults, while NDA method was used for data sets where slip along newly formed fault systems was supposed. The proof of reactivation is initially observed during fieldwork by crosscutting relationships between slip indicators and/or offsetting of older faults by the younger ones. Similar displacements to the latter are distinguished in remote sensing footage or geological maps of the area. The final control of reactivation is performed after attempted

Table 1: Results of stress tensor inversion based on fault-slip data. The field "Fluct. total" represents the mean (per solution, i.e. tensor) angular deviation of the calculated maximum shear stress in the fault plane from the measured slip indicators.

Name	Method	Main stress axes						Datasets			Fluct. total	R	Regime	Quality
		σ_1		σ_2		σ_3		used	total	%				
K01	NDA	27	20	245	64	122	14	11	11	100	8.2	0.91	transtension	c
M01	INV	352	7	234	74	83	13	13	13	100	1.8	0.12	transpression	c
M02	NDA	4	4	206	85	94	1	4	4	100	1.3	0.49	strike-slip	e
M03	INV	18	2	248	85	108	3	9	9	100	1.0	0.79	transtension	d
G01	INV	342	16	196	70	75	10	12	13	92.31	4.2	0.36	strike-slip	c
G02	NDA	177	25	351	63	86	2	11	11	100	7.2	0.48	strike-slip	c
G03	NDA	43	8	293	66	136	21	24	24	100	8.9	0.46	strike-slip	b
G04	NDA	16	12	181	77	286	3	8	8	100	3.9	0.50	strike-slip	d
G05	INV	347	11	228	66	81	20	32	32	100	8.4	0.56	strike-slip	a
R03	NDA	193	16	329	67	99	14	9	9	100	9.6	0.47	strike-slip	d
R02	NDA	216	4	106	76	307	12	21	21	100	8.9	0.52	strike-slip	b
R01	NDA	2	38	172	51	268	4	10	10	100	4.9	0.48	strike-slip	c

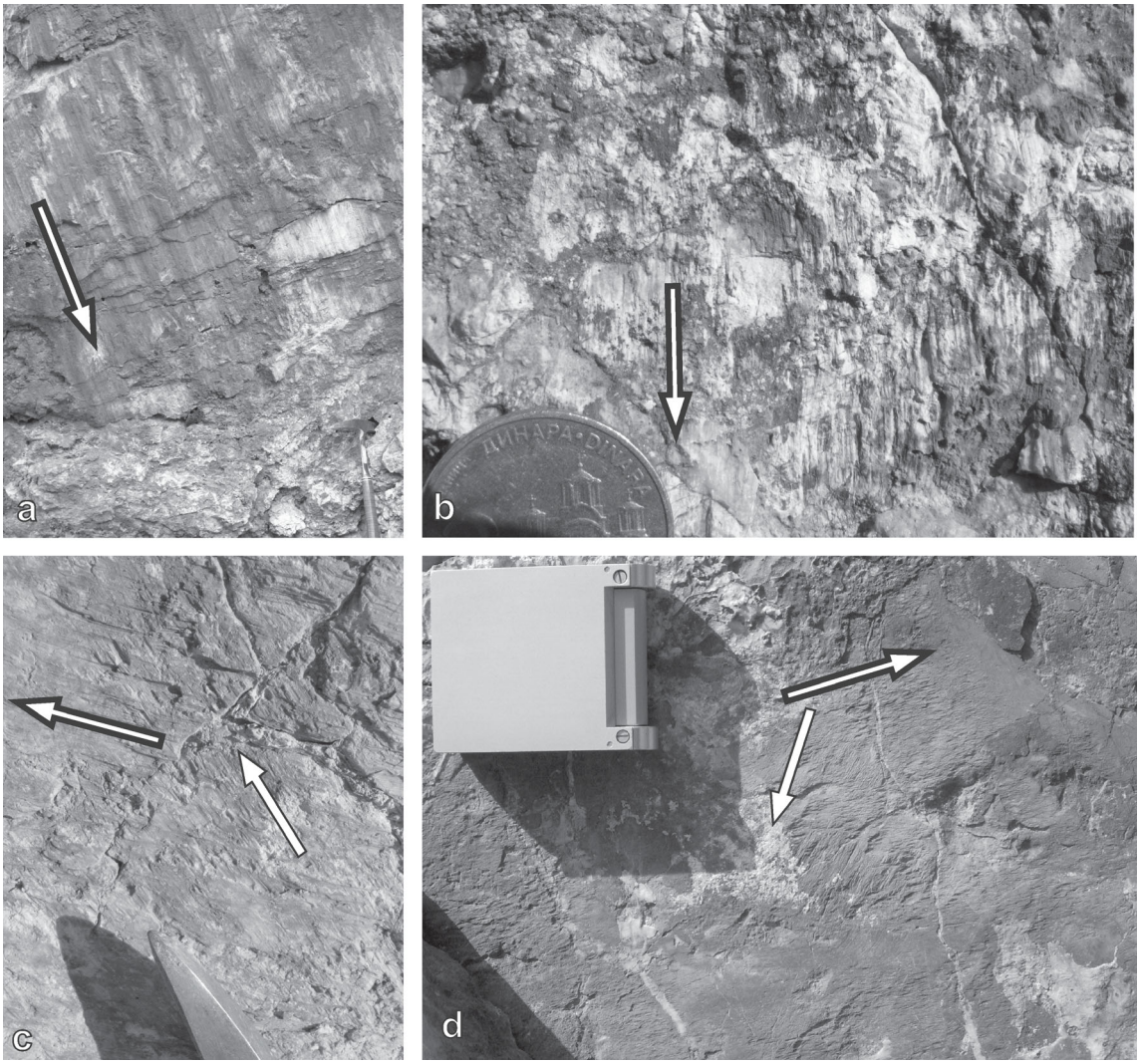

Fig. 4. The most common linear indicators of the youngest tectonic activity. Arrows with thicker lines indicate the youngest phase, while arrows with thinner lines, indicating one of the older phases, were put there to illustrate cross-cutting relationships of the lineations. **a** — Kučevo traverse — kinematic indicators shown as cataclastic lineation and gouging-grain grooves; **b** — Gornjak traverse — most common indicators presented as calcite fibres; **c** — Manasija traverse — the youngest lineation shown as gouging/plucking markings (Doblas 1998); **d** — Ravanica traverse — carrot shaped features indicating the youngest tectonic event.

stress analysis, since reactivated faults plot away from the failure envelope on the Mohr stress diagram. The aim of every inversion is to minimize the deviations between observations and a model. In the case of paleostress analysis deviations between the observed slip and calculated shear stress directions for a given fault-slip dataset should be minimized. As mentioned by Gephart (1990), direction of shear stress is dependent on only four out of six (independent) elements of the stress tensor, thus those four parameters can be obtained using any kind of inversion methods. Three parameters relate to the orientations of the three principal stress axes σ_1 (maximum), σ_2 (intermediate) and σ_3 (minimum), the fourth is the R parameter indicating the relative magnitude ratio between the intermediate principal stress and the two extreme ones $((\sigma_2-\sigma_3)/(\sigma_1-\sigma_3))$.

All data for fault slip analysis were divided into 12 blocks — stations along profiles, where data collecting has been performed (shown on Fig. 5). The general approach involved the analysis of local tensors for detecting potential differences in their orientations. Since the data were generally consistent for the whole area, stress tensors are presented and discussed per field traverse.

The quality assessment of the results was done using the updated quality ranking system of the World Stress Map release 2008 (Heidbach et al. 2008). It involved applying the lowest quality rank criteria among the following ones: the total number of initial data-sets considered for calculations, the percentage of used data-sets in the final calculation against the total number of data, confidence rank based on field observations, fluctuation angle between the calculated slip and the slip observed on the outcrop, and the confidence rank related to the type of the slip indicator used to determine the sense of shear in the field (see Table 1). The overall quality of each result of stress tensor inversion was assigned

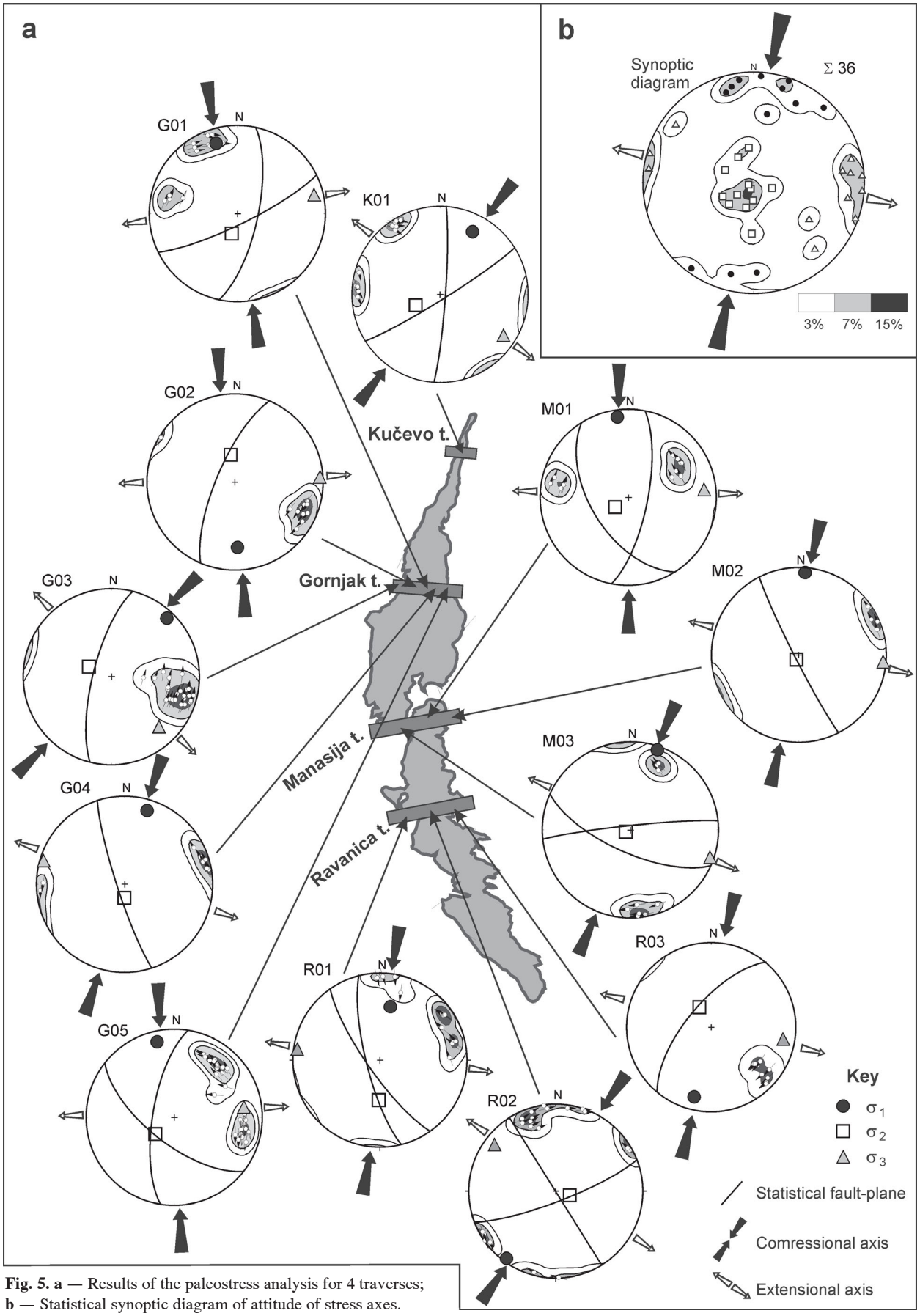

Fig. 5. a — Results of the paleostress analysis for 4 traverses; **b** — Statistical synoptic diagram of attitude of stress axes.

according to the World Stress Map quality ranking scheme and ranges from 'a' (best) to 'e' (worst) (Sperner & Zweigel 2010).

Focal mechanism stress inversion

Focal mechanisms were calculated using the polarity of first arrivals of P waves. Parameters of mechanisms were defined by a double couple model with the velocity model defined by Glavatović (1988). The data on first arrivals were acquired from all available stations in bulletins of the International Seismological Centre (ISC, 2011). The earthquakes used in this study range in magnitude between 2.2 and 4.6 (Table 2). A weak seismicity in the research area as well as a poor seismological network in the region prior to 2000 has limited the data base to only 25 focal mechanisms. As it can be seen in Table 2, all focal mechanisms of earthquakes from the 1980s and 1990s were calculated only for higher magnitude events (M > 3). This was done in order to ensure that the same quality rank could be assigned to these solutions as for the solutions of events after 2000.

Based on the position of epicenters of the studied earthquakes three areas with higher seismic activity could be distinguished. These are: the northern (corresponds to traverse Kučevo), the central (Gornjak and Manasija) and the southern (Ravanica) area (see Fig. 3 and Table 3).

According to Barth et al. (2008), the main deficiency of this method of calculating the focal plane solutions is that the orientation of the principal stress axes cannot be obtained directly. By this method, one can obtain two nodal planes which separate quadrants with dilatational or compressional first P-waves arrivals. Inside these quadrants axes of maximum shortening and maximum dilatation are located. These are P and T axes, respectively, and they represent principal strain axes, which (in most cases) do not coincide with the principal stress axes. Therefore, in order to obtain the orientation of the stress axes, inversion of focal mechanism data had to be done.

There are several methods developed for calculating the stress tensor based on focal mechanism data (Angelier 1979; Gephart & Forsyth 1984; Michael 1987; Rivera & Cisternas 1990; Angelier 2002). In this paper we performed a formal stress inversion of focal mechanisms, following the technique of Gephart and Forsyth (1984). This technique is linked to two main assumptions: (1) the chosen focal mechanism solution lies in a region with a uniform stress field that is invariant in space and time, and (2) the directions of earthquake slip and of maximum shear stress are the same (Wallace–Bott hypothesis; Bott 1959). Result of this inversion technique is a deviatoric stress tensor with definite orientations of the three principal stress axes and the ratio R.

Table 2: Focal mechanism solutions for studied earthquakes (azimuth and dip angle in form dip direction/dip).

Label	Date	X	Y	M	H	Az NP1	Dip NP1	Az NP2	Dip NP2	Az P	Dip P	Az T	Dip T
KB101	27.01.1983	44.08	21.63	3.9	10.0	302	83	152	8	118	52	306	38
KB102	27.05.1988	44.15	21.53	4.4	13.4	327	51	104	48	306	2	212	67
KB103	28.05.1988	44.05	21.71	3.6	10.0	1	48	149	47	253	73	345	1
KB104	09.04.1989	44.27	21.71	3.0	10.0	182	81	280	49	148	21	42	35
KB105	28.10.1991	44.26	21.50	4.6	16.0	10	58	248	49	37	5	135	56
KB106	18.11.1991	44.23	21.50	3.2	10.0	161	63	273	53	129	6	33	48
KB107	16.03.1993	44.10	21.57	2.8	11.0	344	81	246	48	124	36	18	21
KB108	22.04.2003	44.25	21.36	2.9	10.0	128	71	27	63	166	5	260	34
KB109	26.11.2005	43.89	21.69	4.0	16.3	22	59	269	57	55	1	146	49
KB110	28.06.2006	44.54	21.73	3.4	12.9	14	63	258	50	43	7	143	51
KB111	02.07.2006	44.54	21.76	3.1	10.9	283	71	178	55	317	10	56	40
KB112	21.11.2006	43.84	21. 64	4.6	3.6	309	86	40	81	265	3	174	9
KB113	02.12.2006	44.07	21.4	3.7	12.3	218	69	109	49	249	12	352	45
KB114	20.12.2006	44.42	21.74	2.3	16.7	161	83	50	20	320	49	177	35
KB115	20.05.2007	44.03	21.74	3.3	4.1	27	88	296	59	166	23	67	20
KB116	13.02.2008	44.11	21.58	2.3	8.0	181	72	18	18	353	62	185	27
KB117	13.02.2008	44.18	21.66	2.1	2.3	89	73	302	20	253	61	98	27
KB118	22.06.2008	44.5	21.63	2.8	1.0	100	79	346	26	119	30	254	51
KB119	11.01.2009	43.81	21.65	2.2	23.0	346	55	157	35	184	79	342	10
KB120	01.02.2009	44.52	21.65	2.4	3.5	125	89	215	4	309	45	121	45
KB121	08.07.2009	43.88	21.5	2.6	3.1	323	84	53	83	278	1	188	9
KB122	21.11.2010	44.52	21.62	2.1	4.4	304	77	150	14	116	57	309	32
KB123	05.02.2011	44.16	21.70	2.4	3.5	247	80	16	15	237	34	81	53
KB124	20.10.2012	44.5	21.69	3.2	5.0	172	63	278	62	44	41	135	1
KB125	20.11.2012	43.76	21.64	3.2	5.0	336	64	214	43	0	12	109	56

Table 3: Zones/traverses and corresponding earthquakes.

Zone/Traverse(s)	Earthquakes
Northern/Kučevo	KB110, KB111, KB114, KB118, KB120, KB122, KB124
Central/Gornjak and Manasija	KB101, KB102, KB103, KB104, KB106, KB107, KB108, KB113, KB115, KB116, KB117, KB123
Southern/Ravanica	KB109, KB112, KB119, KB121, KB125

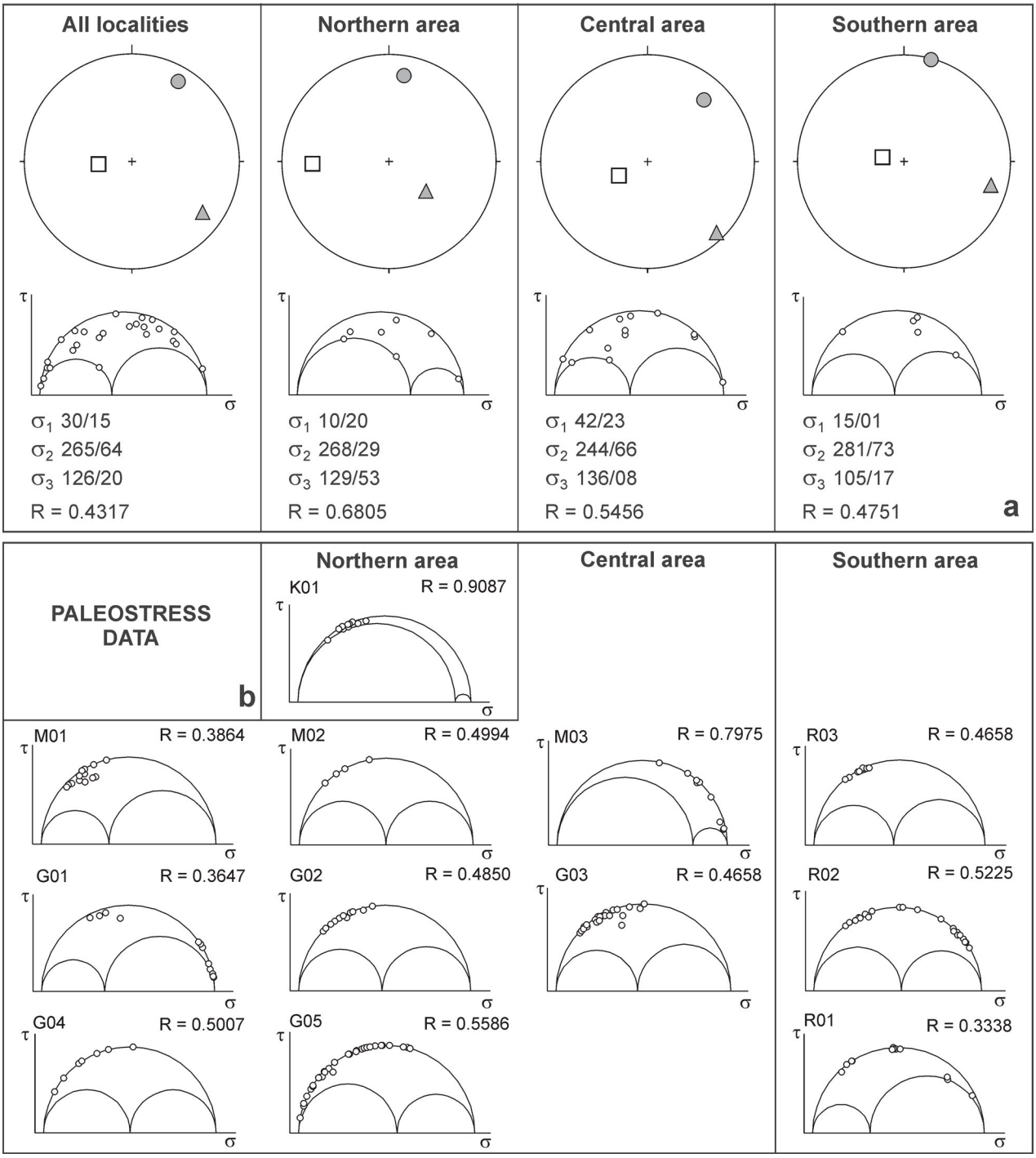

Fig. 6. a — Results of inversion of focal mechanisms data; **b** — Mohr's diagrams obtained by the paleostress analysis.

The quality ranking of the results of the focal mechanism stress inversion (Fig. 6) was carried out according to the scheme applied for fault slip data inversion (Heidbach et al. 2008). It evaluates the azimuthal accuracy of S_{Hmax} obtained by formal inversion of a number of well-constrained single-event focal mechanisms that are located in close geographic proximity (FMF category).

The dip data presented in this paper are displayed as dip direction/dip angle, both for structural and focal mechanism data.

Results

Fault slip analysis

General characteristics of the faults activated by the youngest stress field in the research area are low dip angle of striation and predominant strike-slip movements along the fault planes. The results of fault slip analysis are shown in Fig. 5 and in Table 1.

For the northern part of the study area, in the Kučevo traverse, a single statistical diagram is presented (K01 on Fig. 5). This result features a conjugate system of strike-slip faults which closely resembles dominant lineaments in the Kučevo area observed by satellite imagery (Fig. 3). Stress tensor exhibits strike-slip kinematics with NNE-SSW oriented subhorizontal σ_1 axis (K01 on Fig. 5). The dominant system in this area is represented by NE-SW striking faults. Individual faults of this system exhibit sinistral strike-slip movements along subvertical to vertical fault planes. A concomitant normal component is also recorded and it is most probably due to somewhat steeper dipping shear direction. Relatively steep normal-dextral slip is observed along the N–S striking faults, representing a fault system conjugate to the aforementioned one striking NE–SW.

Along the Gornjak traverse five tensors were distinguished (Fig. 5 and Table 1, tensors named with G-letter). A NNE–SSW striking fault system dominates in most of these solutions, but locally, NW–SE striking fault systems are also observed. The same trends are also observable on a larger scale as regionally important dislocations (Fig. 3). The stress field resulted in sinistral strike-slip movements along the NNE-SSW-striking fault system (e.g. G01, G02 and G05 on Fig. 5). Data-set G03 exhibits a slight deviation from the aforementioned NNE–SSW pattern, exhibiting dextral slip along similarly oriented faults. The remaining fault systems trending NNW–SSE, NW–SE and NE–SW are of local importance (e.g. G05). Along the NNW-SSE and NW–SE systems dextral strike-slip was recorded, while the NE–SW striking faults exhibit sinistral strike-slip. Calculated stress tensors generated strike-slip kinematics with the compressional axis generally directed N–S, locally deviating NNE–SSW (Fig. 5, G03).

Along the Manasija traverse three tensors were distinguished (Fig. 5). Solution M03 reveals the presence of a regionally important ENE–WSW striking system with sinistral slip. There is also a NW–SE system of local importance, which has much steeper reverse-dextral slip. Diagram M01 (Fig. 5) represents a NNE–SSW striking sinistral strike-slip fault system with regional importance. However, a NW–SE system with dextral strike-slip is more frequent on the outcrop-scale. This system can also be observed on the solution M02 (Fig. 5). Calculated stress tensors represent strike-slip kinematics with the NNE–SSW oriented σ_1 axis.

Along the Ravanica traverse, the most important fault systems are generally striking NNW–SSE and NW–SE, as it is shown on diagrams R01 and R02 (Fig. 5). The dominant slips along this system are dextral and locally dextral normal. In this area a significant number of NE–SW striking local faults are observed in the field and also detected by remote sensing lineament analysis. The compressional axis is oriented NNE–SSW.

The synoptic diagram of principal stress axes (Fig. 5b), shows that the general directions of σ_1 and σ_3 are NNE–SSW and ESE–WNW, respectively. Both axes are sub horizontal with a mean dip of 18/08 and 99/06, respectively. The σ_2 axis is steeply dipping in SW quadrant (mean dip 211/81). Any discrepancies of the orientation of main axes result from local perturbations due to stress releases along the reactivated ruptures (i.e. slight obliquity) or inherent inaccuracies during data collection propagated during subsequent correction and paleostress calculation.

Focal mechanisms

The map of the focal plane solutions is given in Fig. 3, whereas detailed information about each solution is reported in Table 2. Correlation between the position of epicenters of earthquakes and the field traverses is given in Table 3. The (re)activation of the faults was determined according to the location of aftershocks, correlation with known regional fault systems and stress inversion.

The focal plane solutions of earthquakes in the northern area (indicated in Table 3) reveal the presence of two general groups of (re)activated faults. The strike of these faults is NNE–SSW and E–W. Two different stress tensors, one transpressional and another transtensional, with two focal solutions corresponding to an almost pure normal slip, can be distinguished. Focal mechanisms labelled KB118 and KB111 show a sinistral slip with an apparent reverse component along the NNE–SSW faults, while solution KB110 shows that this type of slip is also present on the E–W faults. A normal slip occurred along the NNE–SSW faults, which can be seen on the focal plane solutions KB120 and KB122. The focal plane solutions KB114 and KB124, however, indicate sinistral slip with an apparent normal (KB124) and normal slip with a dextral component (KB114) along the E–W faults.

The central area is characterized by the largest number of earthquakes. Focal plane solutions allow the recognizing of three subgroups of fault planes. The first subgroup has a general NNE–SSW strike, it is characterized by either transpressional (KB102, KB106, KB108, KB104) or transtensional tectonics (KB117, KB115, KB101), and has a more or less preferred strike slip component. Faults with this strike were also observed in the field. The field measurements also indicate both dextral and sinistral slips along these fault planes, which is evident along the Gornjak traverse. The second subgroup has a NNW-SSE strike, and, like the previous subgroup, has both transpressional (KB105, KB113, KB123) and transtensional slip (KB107). This subgroup of fault planes is also found in the field, where indications of both reverse and normal slip are observed (field points M02 and G04). The third subgroup of E–W fault planes with almost pure normal slip is found on the focal plane solutions KB103 and KB116. This subgroup is recorded on the field points M03 and G01, where sinistral normal slip is observed.

The focal plane solutions for the southern part of the study area reveal two different fault plane subgroups. The first subgroup (KB109, KB112, KB121 and KB125) has a NW-SE strike. Focal mechanisms for KB121 indicate almost pure sinistral slip, while two others indicate reverse slip both with sinistral and dextral components. The reverse slip was observed in the field on fault planes having the same strike (R01 and R02). However, none of the fault solutions along the Ravanica profile shows a sinistral slip. The third subgroup of fault planes has an ENE–WSW strike and almost pure normal slip, and it is observed on the focal plane solution KB119. This is also confirmed by the diagram R02.

Tensor inversion of focal mechanisms tensor inversion shows that the direction of maximum and minimum stress is NNE–SSW and ESE–WNW, respectively (Fig. 6a), and that in the central and southern area both stress axes are subhorizontal. The σ_2 axis is subvertical in these two areas and in all areas dipping towards the W. The values of the R ratio decrease when going from the northern to the southern parts of the research area.

Discussion

As can be seen in Figures 3, 4 and 5, there is a good correlation of the results among tensor inversion of fault slip data, inversion of focal mechanisms and lineament pattern analysis. This correlation indicates that in the research area the Late Miocene strike-slip tectonic regime (Matenco & Schmid 1999) continued to be active in recent times. This observation coincides with the existing neotectonic interpretations in the Pannonian Basin (Bada et al. 2007), Serbia (south of the Danube and Sava rivers; Marović et al. 2002a) and northern part of the Getic Nappe in the Southern Carpathians in of Romania (Matenco & Schmid 1999; Fügenschuh & Schmid 2005).

Tensor inversion of fault slip and focal mechanism data suggest that the studied area is characterized by subhorizontal compressional and tensional axes as well by subvertical σ_2 axes. This clearly implies a strike slip tectonic regime with a general NNE–SSE orientation of maximum compression. The data also suggest that the compressional axis slightly deviates in the northern and southern part with respect to the central part of the research area (generally N–S oriented maximal axis in both regions). Higher R values (~0.7) in the northern part (Fig. 6), obtained by both methods, indicate a dominant transtensional regime in this area. The shape of the stress ellipsoid tends to have an oblate form ($\sigma_1 \geq \sigma_2 > \sigma_3$) (Fig. 7). This shows differences with respect to the tectonic regime determined for the whole GRZ by this study. The explanation can be twofold: local differences in stress field or the influence of strike-slip tectonics which also

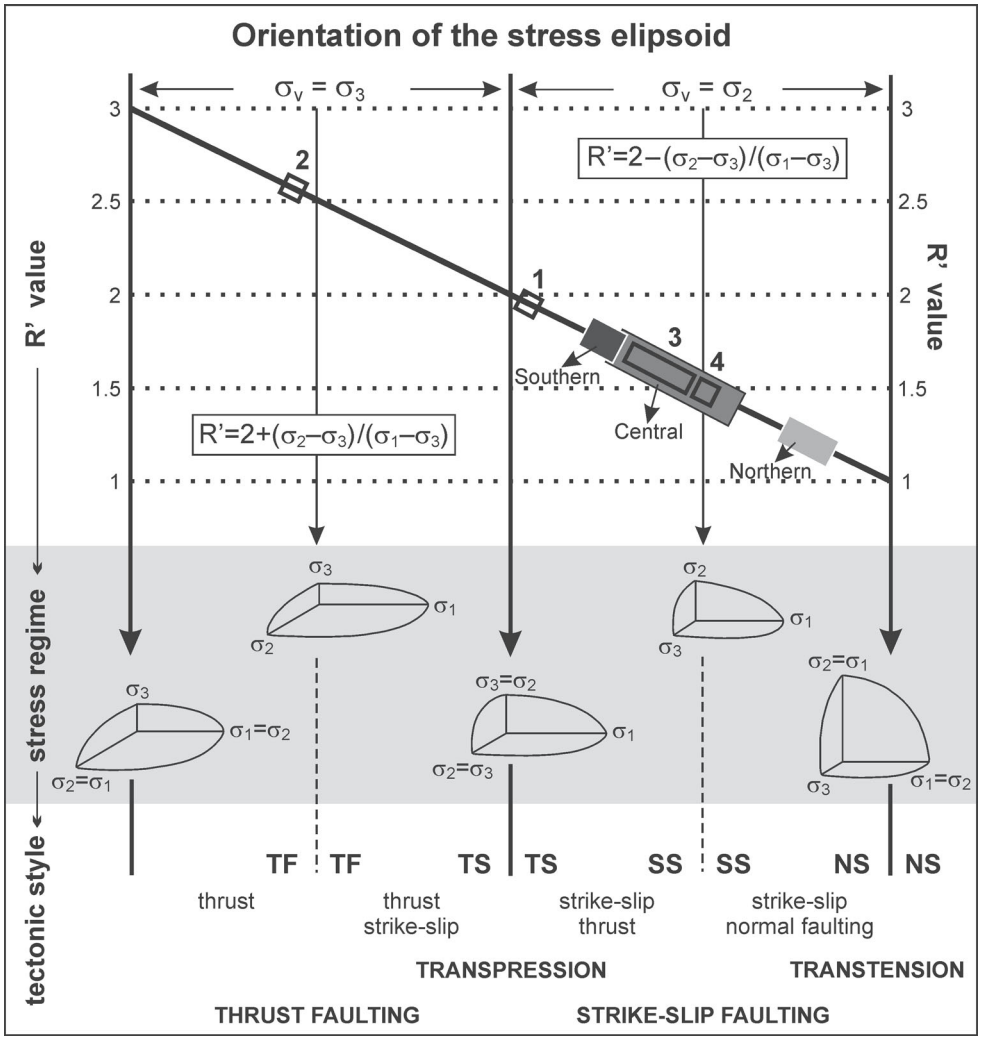

Fig. 7. Diagram of orientation of stress ellipsoid and related tectonic regimes, adapted from Bada et al. (2007). Numbers 1–4 indicate the regions shown on Fig. 8

activated normal faults in the southern Carpathian arc (Schmid et al. 1998; Fügenschuh & Schmid 2005). In the central part of the research area the average R value obtained by both methods (Fig. 6), together with the position of stress field axes (the medium stress axis is subvertical, and the other two subhorizontal), implies a dominating strike-slip regime. R values and the position of principal axes in the southern part of the research area imply a tendency towards a prolate stress ellipsoid. Such a stress regime indicates the affinity to transpressional kinematics (Fig. 7).

Epicenter positions indicate that most earthquakes occurred in the central part of the research area, more precisely, in the area between Despotovac and Petrovac (Fig. 3). This does not necessarily imply that this area has higher seismicity (more frequent earthquakes), since the focal plane solutions are calculated only for earthquakes with magnitude higher than 2. On the other hand, this fact cannot be ignored either, especially because it certainly indicates some kind of different seismic activity in this zone with respect to the northern (no stronger earthquakes) and southern part (low concentration of stronger earthquakes) of the study area. There are also some differences regarding fault (re)activation patterns in the northern and the central part on the one hand, and the southern part of the research area on the other. Earthquakes from the northern and the central part of the research area occurred along generally N–S striking regional faults. By contrast, earthquakes from the southern part occurred along faults that are marked as local on the lineament trend interpretation.

Our results support the model of the "Adria push" mechanism, according to which the maximum compressional stress has a NE–SW orientation, generated in this way in the southern Dalmatia region (Croatian coast, Dubrovnik — Split region) (Figs. 7 and 8) (Rebai et al. 1992; Gerner et al. 1999). As shown by Bada et al. (2007), the azimuth of the σ_1 axis is N055° in the Timisoara seismogenic zone. Although situated south of this seismogenic zone, the GRZ shows the same pattern with the maximum compression axis oriented in a similar direction (030/10). Similar σ_1 orientations are found in the Kraishte area in Bulgaria (tensor 3 of the phase D4 in Kounov et al. 2011). According to Bada et al. (2007), dominant active fault systems in the Timisoara Zone display N–S and ENE–WSW strikes, and the same applies to the GRZ where both regional (N–S and NE–SW) and local (NE–SW and NW–SE) faults show evidence of recent activity. In analogy to the Timisoara Zone, this fact indicates that the distribution of the epicenters, as well as of the fault mechanisms, can be explained by the release of accumulated stress at local accommodation zones that are favourably oriented with respect to the active regional stress field. This explains why the maximum horizontal stress axis slightly deviates from the maximum compressional axis generated by the 'Adria push' mechanism (related to the region of southern Dalmatia in Croatia).

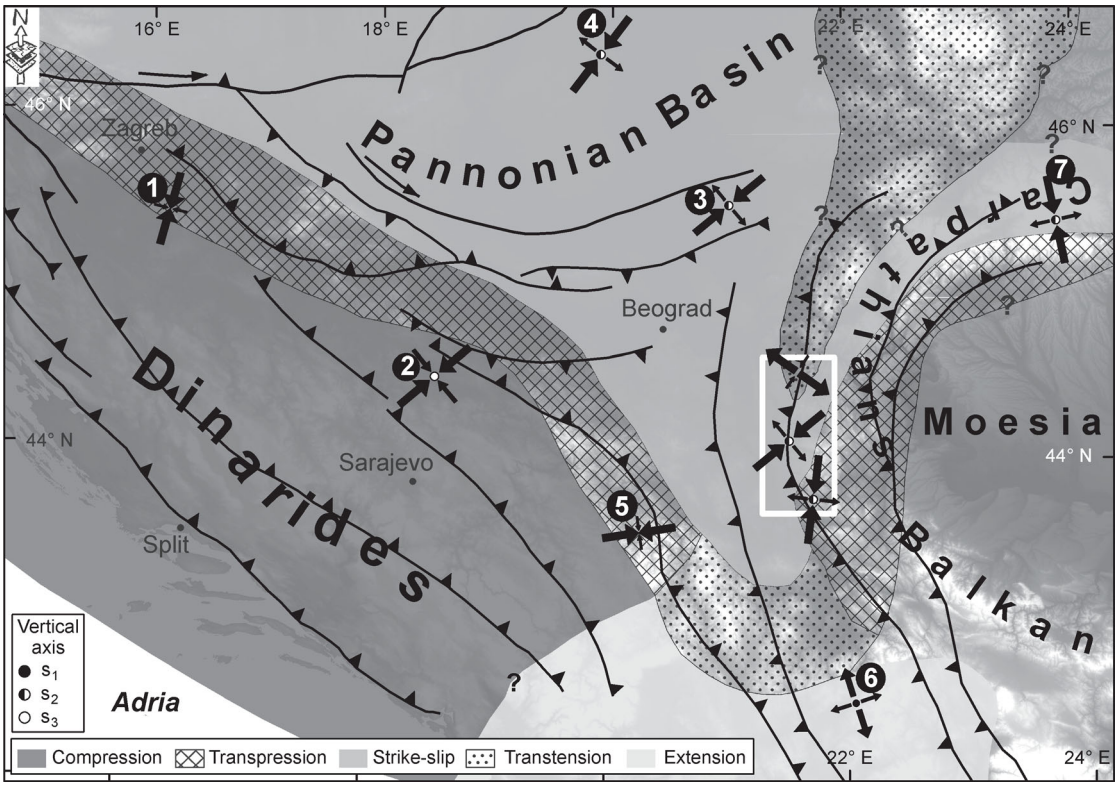

Fig. 8. Schematic map of the recent tectonic stress regimes on the Balkan Peninsula and Pannonian Basin, adapted from Marović et al. (2002a), Radovanović (2003), Fügenschuh & Schmid (2005), Bada et al. (2007), Kastelic et al. (2013). Numbers 1–4 indicates the regions studied by Bada et al. (2007); tensors 5 and 6 are based on research of Marović et al. (2002a); tensor 7 indicate region studied by Fügenschuh & Schmid (2005). The relative size of the presented arrows indicate the relative magnitude of the stress axes, i.e. their mutual ratio. Tensors presented without a circle indicating the vertical axis are solutions where none of the axes were vertical, i.e. transtensional or transpressional.

Observations in the northern and southern parts of the GRZ indicate that the local stress field is of high importance in controlling recent tectonics in this area. The southern part shows the affinity to transpressional tectonics likely influenced by the rigid Moesian Promontory, situated east of our study area (Fig. 8). The northern part is characterized by a transtensional tectonic regime which could mark the onset of the influence of the Pannonian Basin extension (Matenco & Schmid 1999; Fügenschuh & Schmid 2005) (see also Fig. 8).

Conclusions

The correlation and joint inversion of calculated focal mechanism and collected fault slip data led us to the following conclusions related to the Late Miocene to present day tectonics in the Eastern Serbian part of the Carpatho-Balkanides:

1. In most cases, there is a good agreement between (1) the paleostress inversion, (2) the inversion of focal mechanisms and (3) the remote sensing lineament analysis. This fact indicates that the present day stress field is the same as the one that was active in the Late Miocene, meaning that the tectonic stress field has remained relatively uniform since that time.

2. The dominant tectonic stress regime in this area is defined by the NNE–SSW horizontal σ_1, sub-vertical σ_2 and WNW–ESE horizontal σ_3 resulting in strike-slip kinematics along active faults. This is in very good agreement with neotectonic reconstructions in the Pannonian Basin indicating that the basin itself and its southern envelope underwent the same neotectonic evolution.

3. There are differences in tectonic regime in the northern and southern parts of the studied area. The transtensional tectonic regime in the northern part probably resulted from extension that acted more to the north-east of the study area. In the southern part a transpressional tectonic regime was dominant most likely because of the close vicinity of the rigid Moesian Platform. The available data, however, cannot provide a more accurate explanation of these subtle differences in tectonic conditions.

4. The maximum horizontal stress axis has a general NNE–SSW orientation. This implies that the main source of compression in the Balkan Peninsula is 'Adria push' which also represents the major cause of seismicity in the studied area. The seismicity is most likely controlled by the release of accumulated tectonic stress along local weakened zones that are favourably oriented in respect to the active stress field.

Acknowledgments: We thank Alexandre Kounov and an anonymous reviewer for their constructive reviews that significantly improved the paper, and to Dušan Plašienka for his thorough editorial handling. This study was supported by the Serbian Ministry of Education, Science and Technological Development, Projects No. 176016 and No. TR 36009. Ana Mladenović wants to thank the CEEPUS network "Earth-Science Studies in Central and South-Eastern Europe" for support. Vladica Cvetković thanks the Serbian Academy of Sciences and Arts (Project Geodynamics). The authors would like to thank Aleksandar Džunić for stimulating discussions about the seismicity of this area and suggestions on an earlier version of the manuscript. Milan Radovanović is kindly acknowledged for language proofreading.

References

Angelier J. 1979: Determination of the mean principal directions of stresses for a given fault population. *Tectonophysics* 56, 3–4, T17–T26.

Angelier J. 2002: Inversion of earthquake focal mechanisms to obtain the seismotectonic stress IV — a new method free of choice among the nodal planes. *Geophys. J. Int*. 150, 588–609.

ASTER GDEM Project: http://www.jspacesystems.or.jp/ersdac/GDEM/E/index.html

Bada G., Horvath F., Dovenyi P., Szafian P., Windhoffer G. & Cloetingh S. 2007: Present-day stress field and tectonic inversion in the Pannonian Basin. *Global and Planetary Change* 58, 165–180.

Barth A., Reinecker J. & Heidbach O. 2008: Stress derivation from earthquake focal mechanisms. *World Stress Map project*, 1–36.

Bonchev E. 1936: Versuch einer tektonischen Synthese Westbulgariens. *Geol. Balcanica* 2, 3, 5–48.

Bott M.H.P. 1959: The mechanics of oblique slip faulting. *Geol. Mag*. 96, 109–117.

Cvetković V., Prelević D., Downes H., Jovanović M., Vaselli O. & Pécskay Z. 2004: Origin and geodynamic significance of Tertiary postcollisional basaltic magmatism in Serbia (central Balkan Peninsula). *Lithos* 73, 3–4, 161–186.

Dimitrijević M.D. 1963: Sur l'âge du métamorphisme et des plissements dans la masse Serbo-macédonienne. *Bull. du VIe congr. De l'ass. Géol. Carpatho-balkanique, Vol. I. Stratigraphie,* 3, Warszawa and Kraków; *Wyd. Geol.,* Warszawa, 339–347.

Dimitrijević M.D. 1967: Some problems of crystalline schists in the Serbo-Macedonian Massif. *Reports of VIII Congress of CBGA, Petrology and Metamorphism, September 1967*, Belgrade, 59–67.

Dimitrijević M.D. 1995: Geology of Yugoslavia. *Gemini*, Beograd, 1–187 (in Serbian).

Dimitrov C. 1931: Contribution to the geology and petrography of Konyavo Mountain. *Rev. Bulg. Geol. Soc.* 3, 3–52 (in Bulgarian).

Doblas M. 1998: Slickenside kinematic indicators. *Tectonophysics* 295, 187–197.

Doblas M., Mahecha V., Hoyos M. & López-Ruiz J. 1997: Slickenside and fault surface kinematic indicators on active normal faults of the Alpine Betic Cordilleras, Granada, southern Spain. *J. Struct. Geol*. 19, 2, 159–170.

Drew L. 2005: A tectonic model for the spatial occurrence of porphyry copper and polymetallic vein deposits — Applications to the central Europe. *U.S. Geol. Surv. Sci. Report 2005–5272,* 36 p. ISBN 1-411-30960-X

Fügenschuh B. & Schmid S.M. 2005: Age and significance of core complex formation in a very curved orogen: Evidence from fission track studies in the South Carpathians (Romania). *Tectonophysics* 404, 33–53.

Gephart J.W. 1990: Stress and the direction of slip on fault planes. *Tectonics* 9, 4, 845–858.

Gephart J.W. & Forsyth D.W. 1984: An improved method for determining the regional stress tensor using earthquake focal mechanism data: application to the San Fernando earthquake sequence. *J. Geophys. Res*. 89, 9305–9320.

Gerner P., Dovenyi P., Horvath F. & Muller B. 1995: State of recent stress and seismotectonics in the Pannonian Basin and surrounding area. *Terra Abstr*. 7, 1–123.

Gerner P., Bada G., Dovenyi P., Muller B., Onescu M.C., Cloetingh S. & Horvath F. 1999: Recent tectonic stress and crustal defor-

mation in and around the Pannonian Basin: data and models. In: Durand B., Jolivet L., Horvath F. & Serrane M. (Eds.): The Mediterranean Basins: Tertiary extension within the Alpine orogen. *Geol. Soc. London, Spec. Publ.* 156, 269–294.

Glavatović B. 1988: Study of seismicity in the southern Adriatic Sea by simultaneous processing of earthquakes. [Proučavanje seizmičnosti južnog Jadrana simultanom obradom grupe 24 zemljotresa.] *PhD Thesis*, *University of Belgrade, Factulty of Mining and Geology,* Belgrade, 1–213 (in Serbian).

Grenerczy G. & Bada G. 2005: GPS baseline length changes and their tectonic interpretation in the Pannonian Basin. *Geophys. Res. Abstr.*, 7(04808).

Heidbach O., Tingay M., Barth A., Reinecker J., Kurfeß D. & Müller B. 2008: The World Stress Map database release 2008. Doi: 10.1594/GFZ.WSM.Rel2008

Horvath F. & Cloetingh S. 1996: Stress — induced late — stage subsidence anomalies in the Pannonian Basin. *Tectonophysics* 266, 287–300.

International Seismological Centre 2011: On-line Bulletin. *Internat. Seis. Cent., Thatcham*, United Kingdom.
http://www.isc.ac.uk

Kalenić M., Hadži-Vuković M., Dolić D., Lončarević Č. & Rakić O. 1980: Geological map and Guide book for sheet Kučevo (L34-128), Basic Geological Map of SFRY. *Federal Geol. Surv.*, Belgrade, 85 (in Serbian with English abstract).

Karamata S. 2006: The geodynamical framework of the Balkan Peninsula: its origin due to the approach, collision and compression of Gondwanian and Eurasian units. In: Robertson A.H.F. & Mountrakis D. (Eds.): Tectonic development of the Eastern Mediterranean Region. *Geol. Soc. London, Spec. Publ.* 260, 155–178.

Karamata S., Knežević V., Péckay Z. & Đorđević P. 1997: Magmatism and metallogeny of the Ridanj–Krepoljin belt (Eastern Serbia) and their correlation with northern and eastern analogues. *Mineralium Depos.* 32, 452–458.

Kastelic V., Vannoli P., Burrato P., Fracassi U., Tiberti M. & Valensise G. 2013: Seismogenic sources in the Adriatic Domain. *Mar. Petrol. Geol.* 42, 191–213.

Kräutner H. & Krstić B. 2002: Alpine and Pre-Alpine structural units within the southern Carpathians and the eastern Balkanides. *Proceedings of XVII Congress of Carpathian-Balkan Geological Association Bratislava.* ISSN 1335-0552

Kräutner H. & Krstić B. 2003: Geological Map of the Carpatho-Balkanides between Mehadia, Oravita, Niš and Sofia. *Geol. Inst. Serbia*, Belgrade.

Kounov A., Seward D., Burg J.-P., Bernoulli D., Ivanov Z. & Handler R. 2010: Geochronological and structural constraints on the Cretaceous thermotectonic evolution of the Kraishte zone, western Bulgaria. *Tectonics* 29, TC2002.

Kounov A., Burg J.-P., Bernoulli D., Seward D., Ivanov Z., Dimov D. & Gerdjikov I. 2011: Paleostress analysis of Cenozoic faulting in the Kraishte area, SW Bulgaria. *J. Struct. Geol.* 33, 859–874.

Marinković Đ., Nikolić D., Maksimčev S., Bundaleski M. & Vdovijak B. 1978: Map of Tertiary base depths (southern of Sava and Danube). *NTC NIS*, Novi Sad (in Serbian).

Marović M. 2001: Geology of Yugoslavia. *University of Belgrade, Faculty of Mining and Geology,* Belgrade, 1–230 (in Serbian).

Marović M., Đoković I. & Toljić M. 2002a: Neotectonic map of Serbia. *Republic of Serbia, Ministry for the protection of natural resources and environment*, Belgrade.

Marović M., Đoković I., Pešić L., Radovanović S., Toljić M. & Gerzina N. 2002b: Neotectonics and seismicity of the southern margin of the Pannonian Basin in Serbia. *EGU Stephan Mueller Spec. Publ. Ser.* 3, 277–295.

Matenco L. & Schmid S. 1999: Exhumation of the Danubian nappes system (South Carpathians) during the Early Tertiary: inferences from kinematic and paleostress analysis at the Getic/Danubian nappes contact. *Tectonophysics* 314, 401–422.

Michael A.J. 1987: Use of focal mechanisms to determine stress: a control study. *J. Geophys. Res.* 92, 357–368.

Mitchell A.H.G. 1996: Distribution and genesis of some epizonal Zn-Pb and Au provinces in the Carpathian-Balkan region. *Transactions of the Institution of Mining and Metallurgy, Sect. B* 105, 127–138.

Ortner H., Reiter F. & Acs P. 2002: Easy handling of tectonic data: the programs TectonicVB for Mac and TectonicsFP for Windows(TM). *Computers & Geosciences* 28, 1193–1200.

Petit J.P. 1987: Criteria for the sense of movement on fault surfaces in brittle rocks. *J. Struct. Geol.* 9, 5–6, 597–608.

Radovanović S. 2003: Seismic hazard maps and spectra, results of catalogue preparation, seismotectonic modeling and site class definitions. *Proc. of First International Conference, Science and technology for safe development of lifeline systems natural risks: Developments, tools and techniques in the CEI Area, 4–5 November 2003*, Sofia, Bulgaria.

Radovanović S. & Pavlović R. 1992: Some aspects of earthquake generation in the area of Svilajnac–Žagubica. *Ann. Géol. Penins. Balk.* 56, 2, 43–60 (in Serbian).

Radovanović S. & Pavlović R. 1994: Earthquake mechanisms on the Mlava fault. *Ann. Géol. Penins. Balk.* 58, 1, 73–85 (in Serbian).

Rebai S., Philip H. & Taboada A. 1992: Modern tectonic stress field in the Mediterranean region: evidence for variation stress directions at different scales. *Geophys. J. Int.* 110, 106–140.

Reinecker J., Heidbach O., Tingay M., Sperner B. & Müller B. 2005: The release 2005 of the World Stress Map.
(available online at www.world-stress-map.org).

Rivera L. & Cisternas A. 1990: Stress tensor and fault plane solutions for a population of earthquakes. *Bull. Seism. Soc. Amer.* 80, 600–614.

Schmid S., Berza T., Diaconescu V., Froitzheim N. & Fügenschuh B. 1998: Orogen — parallel extension in the South Carpathians during the Paleogene. *Tectonophysics* 297, 1–4, 209–228.

Schmid S., Bernoulli D., Fügenschuh B., Matenco L., Schefer S., Schuster R., Tischler M. & Ustaszewski K. 2008: The Alpine-Carpathian-Dinaride orogenic system: correlation and evolution of tectonic units. *Swiss J. Geosci.* 101, 139–183.

Spang J.H. 1972: Numerical method for dynamic analysis of calcite twin lamellae. *Geol. Soc. Amer. Bull.* 183, 467–472.

Sperner B. & Ratschbacher L. 1994: A Turbo Pascal program package for graphical presentation and stress analysis of calcite deformation. *Z. Dtsch. Geol. Gesell.* 145, 414–423.

Sperner B. & Zweigel P. 2010: A plea for more caution in fault-slip analysis. *Tectonophysics* 482, 29–41.

Ustaszewski K., Schmid S., Fügenschuh B., Tischler M., Kissling E. & Spakman W. 2008: A map — view restoration of the Alpine-Carpathian-Dinaridic system for the Early Miocene. *Swiss. J. Geosci.*, 101, Suppl. 1, S273–S294.

Veselinović M., Antonijević I., Milošaković R., Mićić I., Krstić B., Čićulić M., Divljan M. & Maslarević Lj. 1970: Geological map and Guide book for sheet Boljevac (K34-8), Basic Geological Map of SFRY. *Federal Geol. Surv.* Belgrade, 1–60 (in Serbian with English abstract).

Zagorchev I. & Ruseva M. 1982: Nappe structure of the southern parts of the Osogovo Mts. and the Pijanec region (SW Bulgaria). *Geol. Balcanica* 12, 3, 35–37 (in Russian, with English abstract).